# Measurement of characteristic impedance and wave number of porous material using pulse-tube and transfer-matrix methods

Liang Sun, Hong Hou,[a] Li-ying Dong, and Fang-rong Wan
*College of Marine, Northwestern Polytechnical University, 710072 Xi'an, People's Republic of China*

(Received 31 October 2008; revised 3 June 2009; accepted 7 September 2009)

The time domain implementation of the transfer-matrix method developed by Song and Bolton [J. Acoust. Soc. Am. **107**, 1131–1154 (2000)] for measuring the characteristic impedance and wave number of porous materials is described in this paper. The so called Butterworth impulse is generated in a standing wave tube with a flat frequency response over a wide frequency range. With only two microphone measurements, the transfer matrix of porous layers can easily be determined through the calculation of complex amplitudes of incident, reflected, and transmitted pulses. The procedure has been used to measure the acoustical properties of a fiber material, and good agreement was found between measured acoustical properties and predicted results by Delany and Bazley [Appl. Acoust. **3**, 105–116 (1971)] semiempirical formulas. Although the error associated with the sample-edge constraint still remains, the new method has a better frequency response as a result of the system calibration process, and the optimal inter-microphone distance is no longer required compared to the frequency domain implementation.
 [DOI: 10.1121/1.3242354]

PACS number(s): 43.58.Bh [RR] Pages: 3049–3056

## I. INTRODUCTION

As an effective means of controlling environmental noise, absorptive material and its performance are always of interests to acoustic engineers and scientists. In understanding and evaluating the effects of a material in particular applications, detailed acoustic analyses normally require material properties, such as surface impedance, characteristic impedance, and wave number, or even material macroscopic properties, as the inputs.[1–4] Nowadays determination of these properties still relies on various experimental techniques.

Traditional measurement approaches, and also today's widely adopted approaches for characteristics impedance and wave number determination, include two-thickness,[5] two-cavity methods,[6–9] both of which are carried out in an impedance tube, also known as the standing wave tube. Basically it requires two separate measurements on the surface impedance of the material sample either with different thicknesses or different backing spaces. Many papers have been published with regard to the limitation, error analysis, improved data acquisition, and post-processing techniques based on the two methods.[7] Song and Bolton[10] gave a thorough and comprehensive review on the development history of the technology in their paper.

In the same paper, however, Song and Bolton[10] presented a new measurement approach that was developed based on the transfer-matrix theory. By utilizing the reciprocal principle naturally imposed to the material sample, the characteristic impedance and the wave number are related to the amplitudes of the four approaching waves on both sides of the sample, which successfully eliminated possible variations associated with mounting two samples in the whole process, possible errors induced by insufficient differences in the surface impedance between two thicknesses due to high flow resistivities, and errors for those high dissipative materials of which the surface impedance is not sensitive to backing conditions. Although it was made clear that the method does not apply to elastic porous materials, such as foam, because of the formula taken in transfer-matrix elements, testing result shows promising correlation with Delany and Bazley's empirical predictions for fiber materials that can be considered to be either limp or rigid.[10]

It is worth noting, however, that in these methods, data acquisition and processing were mostly done in the frequency domain, which inevitably leads to either conducting separate measurements on different sample configurations, or setting up a multi-channel data acquisition/processing system. The transfer-matrix method described in Ref. 11 needs four microphone measurements to retrieve the amplitudes of four approaching waves in the standing wave tube. In addition, an optimal inter-microphone spacing should be honored for a given frequency range of interest.

Recently, Jing and Fung[12] developed an impulsive sound source, which can generate repeatable sharp pulses with durations as short as 0.5 ms. Hou and co-workers[13,14] used the echo-pulse tube to measure the absorption coefficient of porous materials through the generation of a kind of pulse referred to as Butterworth pulse. The measurement was conducted in the time domain and in a way that the incident and the reflected pulses could be separated from each other such that the amplitude of each wave can be determined.[15] The technique was claimed to be an effective approach for *in situ* sound absorption coefficient measurements.

[a]Author to whom correspondence should be addressed. Electronic mail: houhong@nwpu.edu.cn

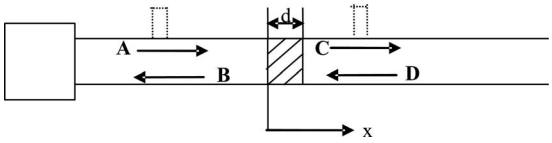


FIG. 1. Schematic of the echo-pulse tube.

The work presented here basically lies within the framework established by Song and Bolton.[10] The transfer-matrix representation of a porous material layer is still limited to be either limp or rigid. The echo-pulse technique is employed to directly measure the amplitudes of four approaching waves, which only requires two microphone measurements. For a chosen fiber material, the complex characteristic impedance and the complex wave number are extracted and compared to those predicted using the Delany and Bazley empirical model. It appears that the approach is able to deliver reliable measurements, and results are even more robust to the tube end conditions.

## II. MEASUREMENT PRINCIPLE

Detailed transfer-matrix analysis can be found in Ref. 10. For a homogeneous, isotropic porous material layer that can be represented by what Allard described as the limp or rigid frame model, there is

$$\begin{bmatrix} T_{11} & T_{12} \\ T_{21} & T_{22} \end{bmatrix} = \begin{bmatrix} \cos k_p d & i\rho_p c_p \sin k_p d \\ i \sin k_p d/\rho_p c_p & \cos k_p d \end{bmatrix}, \tag{1}$$

where $T_{ij}$ is the transfer-matrix elements; and $c_p$, $k_p$, and $\rho_p$ are complex sound speed, complex wave number, and the complex density of the material, respectively. In here, $T_{ij}$ is related to the sound pressures $P$ and normal acoustic particle velocities $V$ on the two surfaces of material layer as

$$\begin{bmatrix} P \\ V \end{bmatrix}_{x=0} = \begin{bmatrix} T_{11} & T_{12} \\ T_{21} & T_{22} \end{bmatrix} \begin{bmatrix} P \\ V \end{bmatrix}_{x=d}, \tag{2}$$

where $x=0$ and $x=d$ denote the two surfaces of the material sample, as shown in Fig. 1. Since $P$ and $V$ at $x=0$ and $x=d$ can also be expressed as the superposition of the four approaching waves in the tube, we have

$$P|_{x=0} = A + B, \quad V|_{x=0} = \frac{A-B}{\rho_0 c_0},$$

$$P|_{x=d} = Ce^{-ikd} + De^{ikd}, \quad V|_{x=d} = \frac{Ce^{-ikd} - De^{ikd}}{\rho_0 c_0}, \tag{3}$$

where $A$, $B$, $C$, and $D$ are complex amplitudes of incident wave, reflected wave from the sample, transmitted wave, and reflected wave from the tube termination, respectively. $\rho_0$ is the ambient fluid density and $c_0$ is the ambient sound speed. With established four equations in Eq. (3), each transfer-matrix element $T_{ij}$ can be expressed as a function of $A$, $B$, $C$, and $D$. Thus if the complex amplitudes of four approaching waves can be determined experimentally, the complex wave number and the characteristic impedance can be extracted through

$$\rho_p c_p = \sqrt{\frac{T_{12}}{T_{21}}}, \tag{4}$$

$$k_p = \frac{1}{d}\cos^{-1} T_{11} \quad \text{or} \quad k_p = \frac{1}{d}\sin^{-1}\sqrt{-T_{12}T_{21}}. \tag{5}$$

When a pulse is generated in a tube and propagates in the $x+$ direction toward the sample as the incident pulse ($A$), the first reflection will happen at the sample surface at $x=0$, and a reflected pulse ($B$) will be generated and propagates in the $x-$ direction. Meanwhile, the transmitted pulse ($C$) will be through the sample surface at $x=d$ and propagates along the $x+$ direction. This pulse will be reflected at the end of the tube as the second reflected pulse ($D$) unless an anechoic end condition is presented. Using $M_1$ and $M_2$ as two fixed reference locations in the upper and down streams of the sample, it can be expected that there would be a delay in the time domain between the incident pulse and the first reflected pulse passing through location $M_1$ and that between the transmitted pulse and the second reflected pulse through location $M_2$. If the pulse is short enough in width, the distance between location $M_1$ and the sample surface $x=0$, and the distance between $M_2$ and the tube end are long enough, the incident and the first reflected pulses can be well separated from each other, and so can the transmitted and the second reflected pulses be. As such, the amplitude of each wave can be determined without much difficulty given today's signal processing technology. It can be seen that this measurement approach only needs two microphone measurements at $M_1$ and $M_2$. As long as the pulses are well separated, the end condition of the tube would not impose any influence on the testing results. For all the testing results shown in this paper, the tube end was left open without any particular acoustical treatments.

## III. EXPERIMENTAL PROCEDURE

Figure 2 shows the experimental setup for the measurements, which includes a standing wave tube, a speaker-pipe system, an NI DAQ6062E data acquisition board controlled by a computer, a BNC2029 adaptor, a power amplifier, and a pre-amplifier. The speaker system is a 5 in. Hi-Vi mid-frequency woofer positioned inside a steel cylinder of which the length is 15 cm. The sound wave from the speaker is guided through a 20 cm long conical reduction to a straight standing wave tube of 27 mm in diameter. The material sample is placed at 72 cm from the end of the tube, and 68 cm away from the speaker. Two measurement locations were chosen at 42 cm away from the sample for $M_1$, and at 25 cm away from the tube end for $M_2$. In the testing, only one microphone, a $\frac{1}{4}$ in. MPA416 condenser microphone, was used to record the data at two locations separately. The analogy input (AI) and analogy output (AO) channels of the NI DAQ 6062E board are programed to be synchronized and have the sampling rate of 100 kHz.

In Ref. 14, it has been shown that the so called Butterworth pulse is considered to be good for acoustic measurement because of its regular waveform, short duration, and

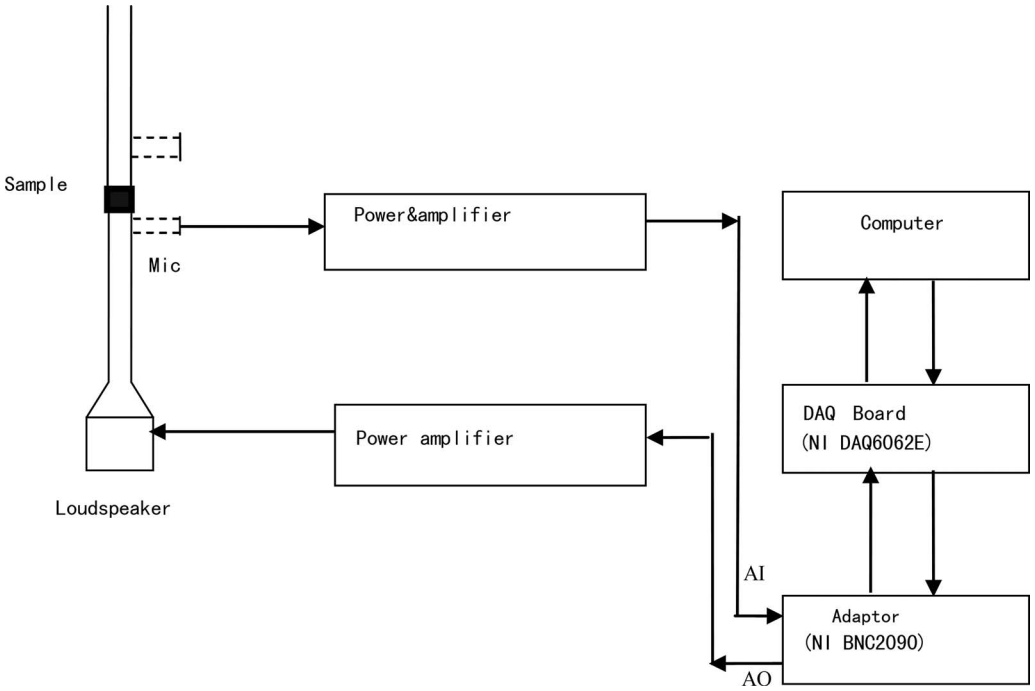


FIG. 2. Sound source configuration and test equipment.

wide frequency range. In this testing, this pulse was used. Figure 3 shows a typical Butterworth pulse waveform and its corresponding frequency spectrum.

In order to generate a desired acoustic pulse signal in the standing wave tube, the impulse response of the sound generator system, including the speaker, power amplifier, etc., should be calibrated so that the appropriate driving signal could be derived. For this purpose, an impulse of fifth-order Butterworth filter shape with 1 ms duration was fed into the system. The acoustic response signal was recorded by a microphone located in the straight standing wave tube. The frequency response of the sound generation system $H(\omega)$ thus can be obtained by

$$H(\omega) = \frac{H_a(\omega)}{H_e(\omega)}, \tag{6}$$

where $H_e(\omega)$ and $H_a(\omega)$ are the Fourier transforms of the excitation and response signals, respectively. For a given desired spectrum $H_b(\omega)$, which is the Butterworth pulse spectrum in here, the spectrum of the driving signal $H_d(\omega)$ can be computed by

$$H_d(\omega) = \frac{H_b(\omega)}{H(\omega)}. \tag{7}$$

Thus the driving signal in the time domain would simply be obtained through the inverse Fourier transform of Eq. (7).

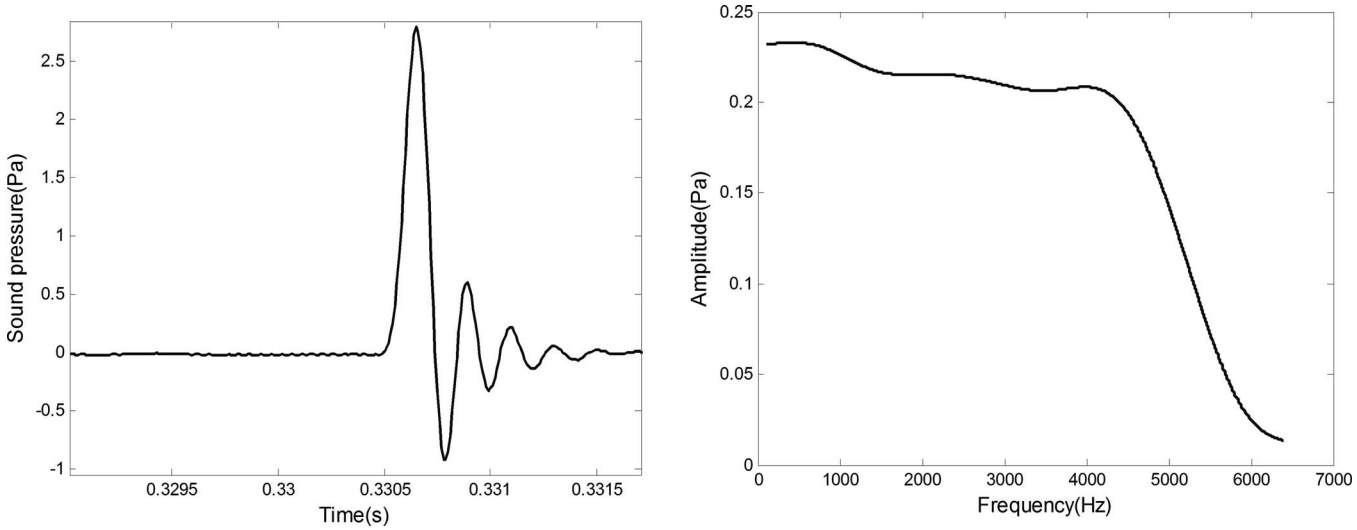


FIG. 3. The Butterworth pulse and its spectrum.

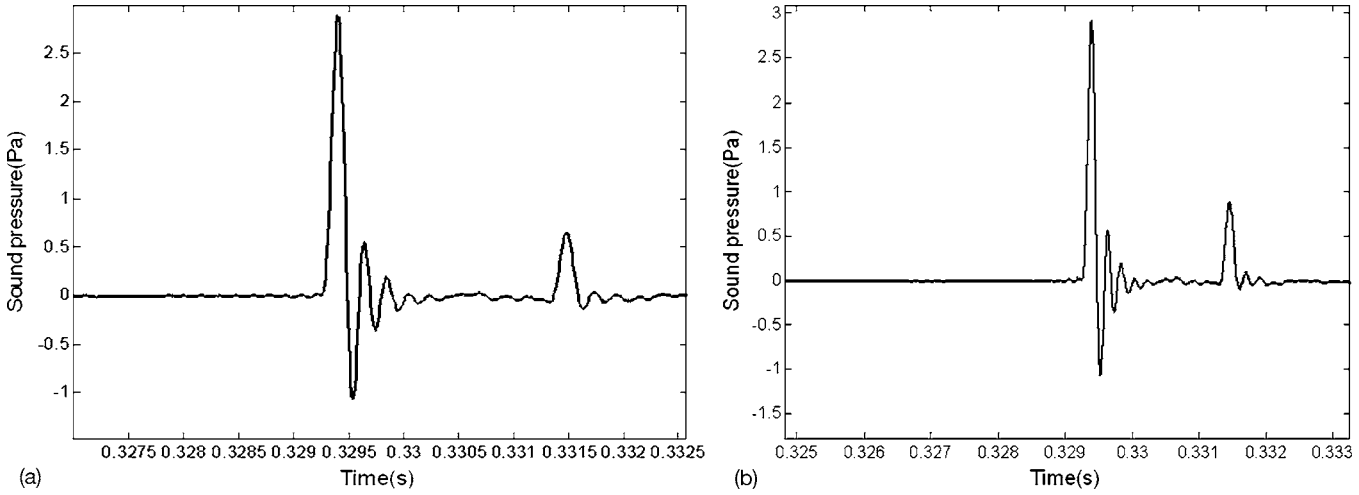


FIG. 4. Measured waveforms of incident and the first reflected pulses with 50 averages.

Compared to traditional methods or Song and Bolton's approach, this process seems to need extra effort in system setups. But for a particular measurement setup, this calibration only needs to be done once. Nevertheless, it should be noted that through this process, any deficiencies in the frequency response of the sound generation system will be compensated, which would improve the signal-to-noise ratio in the measurement.

## IV. EXPERIMENTAL RESULTS

A glass fiber material was chosen for the validation testing. The material bulk density is 24 $kg/m^3$, and the measured flow resistivity is 13 100 Rayls/m. Two samples, 20 and 30 mm in thickness, were prepared. In testing, the pulse width is about 1 ms. For each microphone measurement, the synchronized time signal is averaged through 50 pulse generations to improve the signal-to-noise ratio. Measured waveforms of incident and the first reflected pulses (from the measured sample), transmitted, and the second reflected pulses (from the tube end) with respect to these two samples are shown in Figs. 4 and 5.

Rectangular window was adopted in this work to crop each pulse in the time domain. For each separated pulse, a 65 536 point fast fourier transform (FFT) was then performed to extract coefficients $A$, $B$, $C$, and $D$ in the frequency domain. It should be noted that a successful separation of those pulses basically relies on the time delay between two adjacent pulses passing through the measurement point, which actually depends on the distance between the upstream measurement location and the sample, and that between the downstream measurement location to the tube end. For a pulse of 1 ms in duration, both distances should be greater than 17 cm (assume $c_0=340$ m/s) for two adjacent pulses be distinguished in the time domain. Previous study[14] has shown that as long as the pulses can be separated, very little impact to the final results was found with regard to measurement locations. This can be considered as another advantage over traditional multi-microphone method, which needs to identify the microphone and sample positions precisely.[15]

As a comparison, predictions made by utilizing the Delany and Bazley semiempirical formulas are also plotted.[16]

From Figs. 6–9, the measured complex wave number, complex material density, and the complex sound speed are shown. Good agreement can be seen between the method

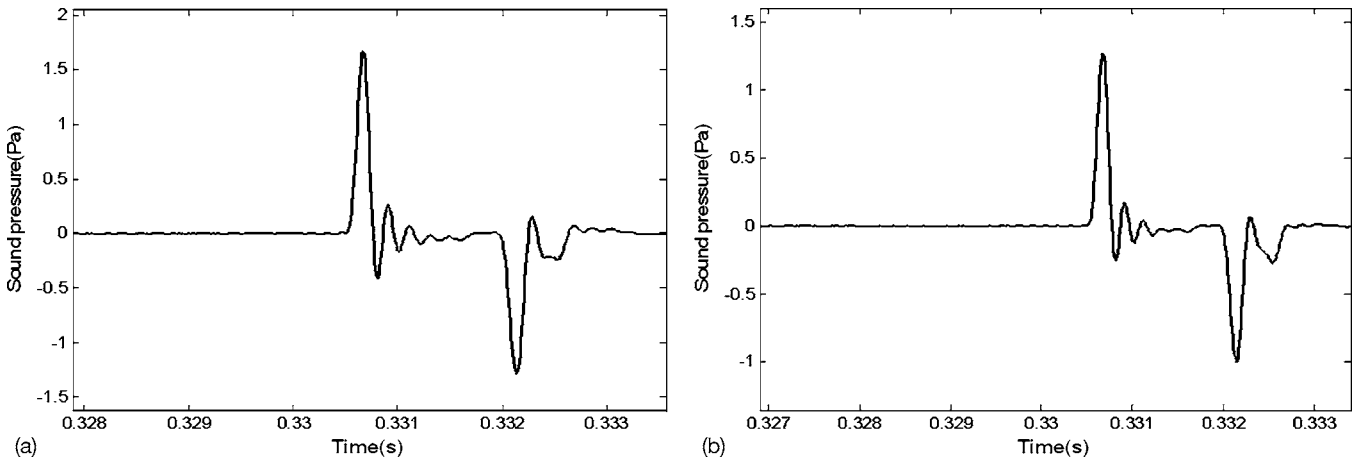


FIG. 5. Measured waveforms of transmitted and the second reflected pulses with 50 averages.

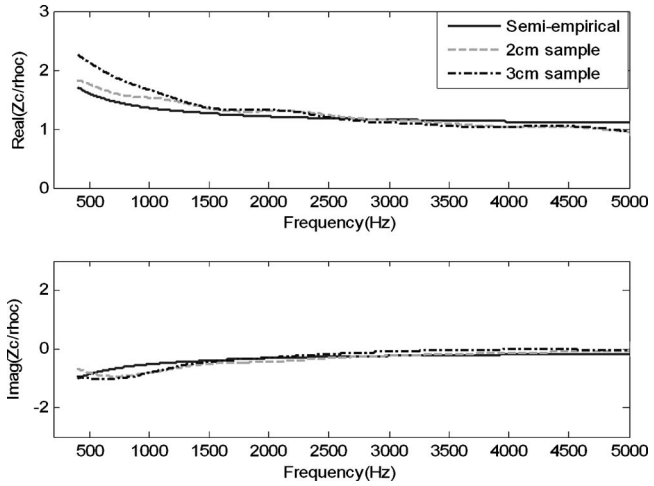


FIG. 6. Normalized characteristic impedance of fiber material determined by using transfer-matrix method and predicted using semiempirical formulas.

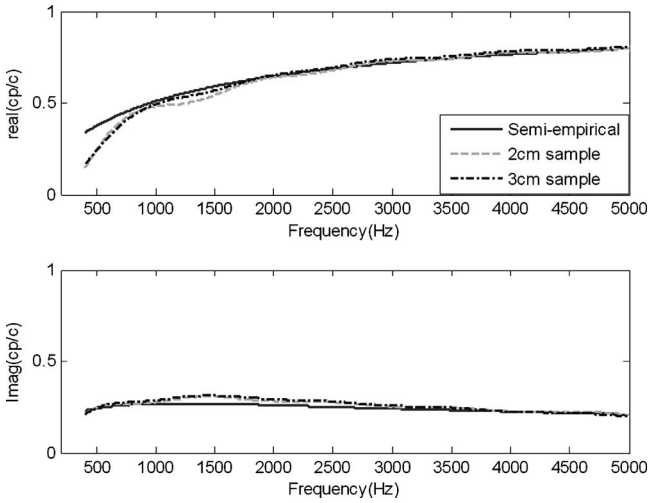


FIG. 8. Normalized complex sound speed of fiber material determined by using transfer-matrix method and predicted using semiempirical formulas.

presented in this paper and predicted results. Also, measured results are irrespective to the sample thickness as expected. Some disagreements occurred at lower frequencies might be related to the sample-edge constraints as discussed in Ref. 10.

## V. SENSITIVITY AND ERROR ANALYSIS

To evaluate our new method correctly, uncertainty analysis of measurement system and computations is presented here followed by some disagreement analysis. From Eqs. (3) and (5), one can see that the calculated characteristic impedance and wave number values are mainly related with the amplitudes of four approaching waves $A$, $B$, $C$, and $D$, as well as the sample thickness $d$, sound speed $c$, and the characteristic impedance $\rho_0 c$ in air, which are closely related to environment temperature. Simulations are therefore made to investigate the impact of uncertainties of above contributors on the estimated characteristic impedance and wave number values. The following values are used in our simulations that are typical in most acoustic laboratories: Variations in amplitudes of all pulses are assumed to be $\pm 1\%$, and uncertainties in sample thickness are $\pm 1$ mm. As sound speed and characteristic impedance of air are affected by ambient temperature, variation is chosen as $\pm 1$ °C.

To analyze the impact of these uncertainties, the Monte Carlo method[17] is employed. For each variable, the Gaussian distribution is adopted with a standard deviation ($\sigma$) defined as above. A random perturbation, which is limited to $\pm 2\sigma$, is then added to the appropriate input variable to calculate the new $Zc$ and $kp$ values. This procedure is repeated until the mean values and standard deviations converge. In our simulations, convergence can be reached after 20 000 iterations. To ensure an accurate result, the analysis was run for 100 000 iterations.

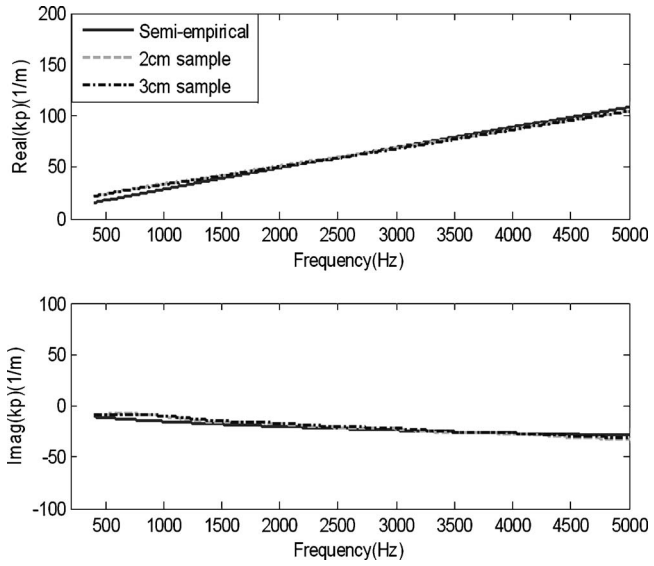


FIG. 7. Wave number within fiber material determined by using transfer-matrix method and predicted using semiempirical formulas.

### A. Errors from measurement system itself

Measuring system can introduce errors in the process of pulse generation, signal sampling, and its conditioning.

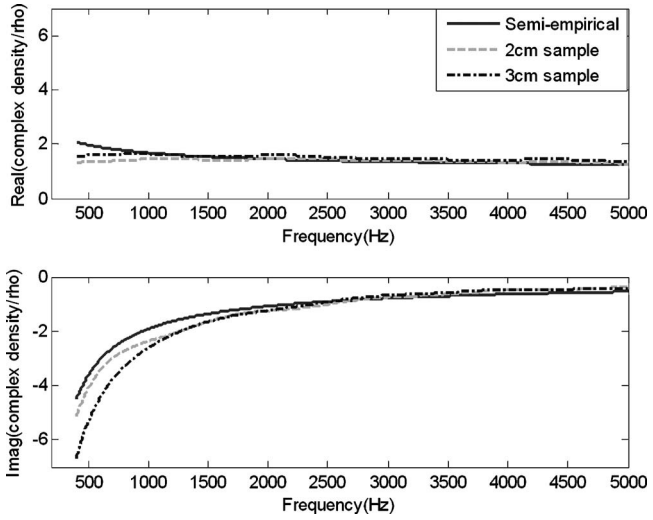


FIG. 9. Normalized complex density of fiber material determined by using transfer-matrix method and predicted using semiempirical formulas.

TABLE I. Effect of amplitude error of incident pulse on calculated results.

| | Frequency (Hz) | | | | |
|---|---|---|---|---|---|
| Error bounds | 400 | 500 | 800 | 1000 | 2000 |
| Re($Zc$) | 1.5% | 1.63% | 0.91% | 0.47% | 0.0429% |
| Im($Zc$) | 2.94% | 2.17% | 1.36% | 1.1% | 0.34% |
| Re($kp$) | 6.08% | 6.06% | 5.2% | 4.26% | 1.66% |
| Im($kp$) | 42.16% | 41.5% | 42.01% | 42.59% | 42.93% |

TABLE II. Effect of amplitude error of reflected pulse on calculated results.

| | Frequency (Hz) | | | | |
|---|---|---|---|---|---|
| Error bounds | 400 | 500 | 800 | 1000 | 2000 |
| Re($Zc$) | 0.25% | 0.19% | 0.25% | 0.32% | 0.30% |
| Im($Zc$) | 0.72% | 0.7% | 0.62% | 0.52% | 0.23% |
| Re($kp$) | 1.72% | 2.07% | 2.42% | 2.16% | 1.16% |
| Im($kp$) | 1.78% | 1.91% | 2.48% | 2.6% | 2.14% |

TABLE III. Effect of amplitude error of transmitted pulse on calculated results.

| | Frequency (Hz) | | | | |
|---|---|---|---|---|---|
| Error bounds | 400 | 500 | 800 | 1000 | 2000 |
| Re($Zc$) | 1.73% | 1.81% | 1.15% | 0.78% | 0.34% |
| Im($Zc$) | 2.22% | 1.48% | 0.75% | 0.57% | 0.10% |
| Re($kp$) | 4.35% | 3.99% | 2.81% | 2.10% | 0.49% |
| Im($kp$) | 40.53% | 39.78% | 39.61% | 40.5% | 40.6% |

TABLE IV. Effect of measurement error in sample thickness on calculated results.

| | Frequency (Hz) | | | | |
|---|---|---|---|---|---|
| Error bounds | 400 | 500 | 800 | 1000 | 2000 |
| Re($Zc$) | 1.65% | 1.38% | 1.11% | 1.06% | 0.39% |
| Im($Zc$) | 1.28% | 1.67% | 1.71% | 1.46% | 1.29% |
| Re($kp$) | 4.33% | 6.15% | 8.08% | 7.41% | 6.31% |
| Im($kp$) | 22.6% | 22.39% | 30.55% | 39.69% | 47.23% |

TABLE V. Effect of measurement error in temperature on calculated results.

| | Frequency (Hz) | | | | |
|---|---|---|---|---|---|
| Error bounds | 400 | 500 | 800 | 1000 | 2000 |
| Re($Zc$) | 0.11% | 0.093% | 0.075% | 0.071% | 0.026% |
| Im($Zc$) | 0.086% | 0.11% | 0.11% | 0.098% | 0.086% |
| Re($kp$) | 0.13% | 0.03% | 0.09% | 0.05% | 0.11% |
| Im($kp$) | 0.22% | 0.25% | 0.28% | 0.26% | 0.12% |

TABLE VI. Effect of all factors on calculated results.

| | Frequency (Hz) | | | | |
|---|---|---|---|---|---|
| Error bounds | 400 | 500 | 800 | 1000 | 2000 |
| Re($Zc$) | 1.54% | 1.29% | 1.04% | 0.99% | 0.37% |
| Im($Zc$) | 1.19% | 1.56% | 1.60% | 1.36% | 1.20% |
| Re($kp$) | 6.34% | 8.61% | 12.08% | 12.41% | 16.4% |
| Im($kp$) | 22.53% | 22.83% | 30.83% | 40.04% | 47.29% |

These errors will appear in the amplitudes of sampling pulses. In this part, amplitudes errors' effects on the final measuring results will be explored.

To simulate the experiment, we use the calculated results of characteristic impedance and wave number implemented by this new method as the baseline values. In the following tables, five frequencies 400, 500, 800, 1000, and 2000 Hz selected randomly are used to study the errors' effect on the final calculated values.

Table I details that error bound is more noticeable in wave number than that of characteristic impedance when amplitude of incident pulse slightly changes. In particular, it can reach an error bound about 42.93% for imaginary part of wave number. Another conclusion can be drawn that amplitude error can affect imaginary parts of $Zc$ and $kp$ more significantly than real parts of them.

It may be seen from Table II that error in reflected pulse amplitude can affect the calculated results slightly with a maximum error bound of 2.6%. Nonetheless, it follows the same rule as shown in Table I that imaginary part can be influenced more significantly than real part of them.

When seen from Table III, it also follows the same rules as indicated in Table I: Imaginary parts of both $Zc$ and $kp$ are significantly affected by the error in transmitted pulse amplitude, and big errors have also been introduced for it over whole frequency range for imaginary part of $kp$. So, it may be concluded that error in transmitted pulse amplitude is also a dominant contributor to the final whole errors.

### B. Measurement error in sample thickness

It is of interest to investigate the impact of sample thickness error on the results of $Zc$ and $kp$. This uncertainty is assumed to be $\pm 1$ mm as 20 mm used as baseline thickness values for all calculations.

It can also be seen from Table IV that complex wave numbers are more sensitive to errors in sample thickness measurement than characteristic impedance. Particularly, the imaginary part of $kp$ would be severely influenced by sample thickness error.

### C. Error in temperature measurement

As our experiment is implemented at the temperature about 15 °C, the values of sound speed 340 m/s and characteristic impedance 415 N s/m$^3$ in air are adopted. At the same time, since they are dominated by temperature, its measurement error is given as $\pm 1$ °C. The following values are utilized: sound speed range 339–341 m/s, corresponding with characteristic impedance varied from 414 to 416 N s/m$^3$. The simulation results are given in Table V.

Table V shows that temperature error impact on final calculated results is negligible in general.

### D. Overall error

From Table VI, one can see that error bounds in characteristic impedance are much smaller than that of complex wave number. Besides this, the error bounds in imaginary part of complex wave number become bigger as frequency increases.

From above analysis, some conclusions can be drawn as follows: (1) The main error contributors result from errors in amplitudes of incident, transmitted pulses as well as in sample thickness; and (2) the effect of temperature measurement error on results can be negligible.

## VI. CONCLUSIONS

The intention of the present work is to further improve the efficiency and accuracy of the transfer-matrix method for determining the fundamental acoustical properties of commonly used porous materials. By employing the echo-pulse technique in a standing wave tube, the microphone measurements can be cut to half compared to the four microphone measurements in the frequency domain implementation described by Song and Bolton.[10] In addition, with the help of impulse response calibration process, the signal-to-noise ratio in the measurement is improved due to a compensated frequency response of the sound generation system. The optimal inter-microphone distance to facilitate a better frequency response is no longer required in this approach as long as the incident, reflected, and the transmitted pulses can be separated. However, it should be noted that possible errors associated with the sample-edge constrain as illustrated in Ref. 10 still remain in the approach presented.

## ACKNOWLEDGMENTS

This work was financially supported by the National Natural Science Foundation of China with Grant No. 10674111 and doctorate foundation of Northwestern Polytechnical University with Grant No. Cx200802. We are grateful to Dr. Chong Wang at General Motors Corporation for his helpful discussions. Our thanks also go to Professor Xiaolin Wang and Mrs. Jie Wang and Mr. Baojun Chang for their help in sample preparations and flow resistivity measurements.

[1]R. A. Scott, "The absorption of sound in a homogeneous porous medium," Proc. Phys. Soc. London **58**, 358–368 (1946).
[2]R. F. Lambert and J. S. Teaser, "Acoustic structure and propagation in highly porous, layered, fibrous materials," J. Acoust. Soc. Am. **76**, 1231–1237 (1984).
[3]L. L. Beranek, "Acoustical properties of homogenous isotropic rigid tiles and flexible blankets," J. Acoust. Soc. Am. **19**, 556–568 (1947).
[4]C. Zwikker and C. W. Kosten, *Sound Absorbing Materials* (Elsevier, Amsterdam, 1949).
[5]M. A. Ferrero and G. G. Sacerdote, "Parameters of sound propagation in granular absorption materials," Acustica **1**, 135–142 (1951).
[6]S. L. Yaniv, "Impedance tube measurement of propagation constant and characteristic impedance of porous acoustical material," J. Acoust. Soc. Am. **54**, 1138–1142 (1973).
[7]C. D. Smith and T. L. Parott, "Comparison of three methods for measuring acoustic properties of bulk materials," J. Acoust. Soc. Am. **74**, 1577–1582 (1983).
[8]H. Utsuno, T. Tanaka, T. Fujikawa, and A. F. Seybert, "Transfer function method for measuring characteristic impedance and propagation constant of porous materials," J. Acoust. Soc. Am. **86**, 637–643 (1989).
[9]A. D. Pierce, *Acoustics: An Introduction to Its Physical Principles and Applications* (McGraw-Hill, New York, 1981).
[10]B. H. Song and J. S. Bolton, "A transfer function approach for estimating the characteristic impedance and wave numbers of limp and rigid porous materials," J. Acoust. Soc. Am. **107**, 1131–1154 (2000).
[11]R. T. Muehleisen, C. W. Beamer, and B. D. Tinianov, "Measurement and empirical model of the acoustic properties of reticulated vitreous carbon," J. Acoust. Soc. Am. **117**, 536–544 (2005).
[12]X. Jing and K. Y. Fung, "Generation of desired sound impulses," J. Sound Vib. **297**, 616–626 (2006).
[13]S. Xu and H. Hou, "A method to develop a dignally-controlled sound impulse generator," Journal of elementary electroacoustics **31**, 9–13 (2007).
[14]H. Hou, S. Liang, D. Liying, and W. Fangrong, "Sound absorption measurement in a circular pipe using echo-impulse method," Acta Metrologica Sinica (in press).
[15]S. H. Jang and J. G. Ih, "On the multiple microphone method for measuring induct acoustic properties in the presence of mean flow," J. Acoust. Soc. Am. **103**, 1520–1526 (1998).
[16]M. E. Delany and E. N. Bazley, "Acoustical properties of fibrous absorbent materials," Appl. Acoust. **3**, 105–116 (1970).
[17]R. T. Muehleisen and C. W. Beamer IV, "Comparison of errors in the three- and four-microphone methods used in the measurement of the acoustic properties of porous material," J. Acoust. Soc. Am. **107**, 112–117 (2002).